Stiffness Mapping: a Dynamic Imaging Technique

Application Note

Bryan Crawford

Introduction

Dynamic imaging, also known as stiffness mapping, on nanoindentation systems is a relatively new technique that expands the capabilities for detecting surface defects and fractures that ordinarily can not be resolved by topographical imaging. The sensitivity in the measurement of stiffness to small changes in contact area enables a technique that provides stark contrast in surface features. Using the measured stiffness data and assuming the applicability of Hertz's assumptions for elastic contact theory, these stiffness maps can also be converted into mechanical properties maps for properties such as elastic modulus. This article carefully examines the assumptions associated with Hertz's elastic contact theory and details how a stiffness map, collected through contact scanning, can be converted into an elastic modulus map. It is shown that, while it is theoretically possible to convert a stiffness map into a mechanical properties map, the assumptions are numerous and often invalid for most interesting samples. Carbon fiber and fused silica samples are used in this article for detailing the value of dynamic imaging for the detection of surface features that ordinarily cannot be imaged using standard scanning techniques of nanoindenter systems.

Samples

Analysis of the elastic equations that describe the onset of plasticity for spherical indentation – discussed in detail in the next section – show that the ideal sample for analysis by stiffness mapping has a high yield stress to elastic modulus ratio; the normal force at the onset of plasticity is proportional to the yield stress divided by the elastic modulus squared. Therefore, a material with a low elastic modulus and high yield strength will result in a stiffness map that is minimally affected by plasticity. A sample that meets this criterion is a carbon fiber composite. The carbon fiber composite sample used in this article is a low modulus high-tensile strength carbon fiber embedded in an epoxy matrix. Carbon fibers of this type typically have an elastic modulus <100 GPa and a tensile strength >3 GPa [1]. The sample was metallographically mounted and polished by the supplier and is shown on the left in Figure 1.

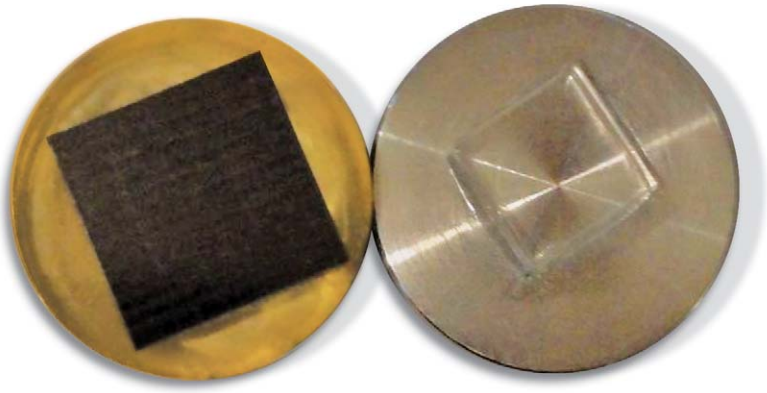

Figure 1. Carbon fiber composite (left) and fused silica (right) samples used in the demonstration of stiffness mapping.

The second sample tested was fused silica which is shown on the right in Figure 1. A major benefit of the stiffness mapping technique is in detecting small changes in contact area. Stiffness measurements change dramatically when surface roughness is encountered due to tip contact on peaks or in valleys. While stiffness imaging on samples even with moderate levels of surface roughness will produce convoluted images of topography, plasticity, and material properties changes that cannot be decoupled, stiffness mapping can be used as an advantage when examining fracture in samples and measuring the length of crack propagation. Fused silica is used in this article to evaluate the advantages of observing crack propagation length using stiffness mapping.

Test Methodology

All of the tests were conducted on the Agilent Nano Indenter G200 using the Dynamic Contact Module (DCM), Nano Vision, and the Continuous Stiffness Measurement (CSM) option. The DCM transducer is ideal for applications involving ultra-low loads and requiring ultra-high displacement resolutions. In addition, the higher resonant frequency and lower damping of this transducer allows higher operating frequencies when scanning to produce stiffness maps. The Nano Vision option enables imaging through the use of a high precision peizo translation stage; lateral resolutions and flatness of travel is better than 2 nm. This system provides quantitative imaging and high precision targeting for the investigation of material properties. Harmonic displacements and harmonic loads were generated during stiffness mapping using the CSM option. In standard applications, the CSM option provides the means for measuring the evolution of mechanical properties as a function of penetration during an indentation test. However, in this application the CSM option is used for applying a harmonic displacement oscillation while the tip scans the surface of the sample and measures the stiffness of the contact to produce a stiffness map of the scanned area.

Four primary steps are used for generating a stiffness map. First, the tip is engaged with the sample and a user defined minimum scan load is applied; the minimum scan load usually ranges between 0.5 µN and 6 µN based on the level of surface roughness that is being scanned. Following the application of the minimum scan load, an oscillatory harmonic displacement of approximately 1 nm at 400 Hertz is applied and the software automatically calculates the standard deviation in the harmonic displacement signal. If the minimum scan load is too small to generate an elastic contact that is able to support the 1 nm harmonic oscillation, then the scan load is incremented until the standard deviation of the harmonic displacement becomes less than 5% of the oscillation size; when the scan load is too small this causes erratic control of the harmonic displacement as the indenter tip "wood-peckers" the surface of the sample [2]. Following stability of the harmonic displacement oscillation, the sample area is scanned while the stiffness of the contact is continuously calculated using Equation 1.

$$S = \frac{F}{h} \cos \varphi \qquad (1)$$

Where S is the stiffness of the contact, F is the applied harmonic force, h is the resulting harmonic displacement, and φ is the phase angle between the harmonic force and the displacement response signals.

The scan speed is automatically calculated based on the selection for scan resolution. A resolution of high, medium, or low is selected by the user along with inputting the number of data points to be collected in each scan line. The resolutions of high, medium and low each correspond to the number of harmonic waves that are collected for each data point; the resolutions correspond to 50, 30, and 20 waves of data, respectively. When calculating stiffness using dynamic techniques, the more waves of data that are collected at each point results in higher accuracies in the stiffness measurement allowing the differentiation of smaller stiffness changes in the material. The scan speed takes into account the frequency of operation (harmonic frequency), the set resolution (waves of data), the number of data points per scan line (number of data points), and the scan distance using Equation 2.

$$Scan\ Speed = \frac{Harmonic\ Frequency}{Waves\ of\ data} \times \frac{Scan\ Distance}{Number\ of\ data\ points} \qquad (2)$$

Equation 2 calculates the number of data points that are to be scanned per second and multiplies it by the distance between each point. Using this technique typical low resolution scans can be performed in less than 15 minutes while high resolution scans take approximately 45 to 75 minutes, based on a 25 X 25 µm scan area.

Can a stiffness map that is obtained from contact scanning be converted into a mechanical properties map?

When the stiffness map of an area is completed, it is very tempting to perform a direct conversion of the stiffness map to a mechanical properties map using Hertz's elastic contact theory. In making this conversion, the fundamental assumptions of Hertz's elastic contact theory should be carefully analyzed. These assumptions are listed by K.L. Johnson but are also provided here [3].

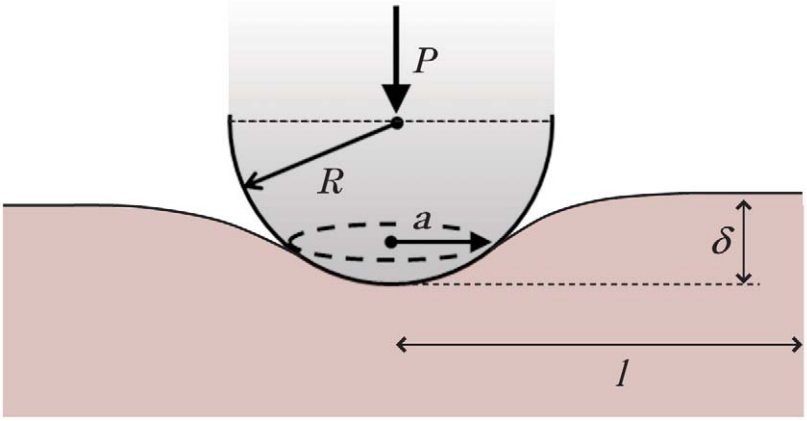

Figure 2. Diagram of the contact between a spherical indentation tip and a sample.

1) The surfaces are continuous and non-conforming: $a \ll R$;
2) The strains are small: $a \ll R$;
3) Each solid can be considered as an elastic half-space: $a \ll R_{1,2}, a \ll l$;
4) The surfaces are frictionless: $q_x = q_y = 0$.

Where a is the radius of contact, R is the radius of the tip (note that the radius of a flat sample is $R_2 = \infty$), l is the length of the sample to boundaries, and q_x and q_y are the tangential forces that give rise to friction. The contact between a spherical tip and a sample is diagramed in Figure 2.

If all four of these criteria can be met, then Hertz's elastic contact stress formulae may be used to determine the contact area, giving rise to the necessary data relationships (load, displacement, and area) needed to determine mechanical properties. In doing this, first, the measured stiffness must be corrected for the stiffness contribution from the test instrument using Equation 3.

$$S = K_f + K_s \tag{3}$$

Where S is the measured stiffness, K_f is the stiffness contribution due to the instrument (frame), and K_s is the contact stiffness of the tip-sample interaction.

Second, Hertz's formula for the radius of contact, shown in Equation 4, can be substituted into the Equation 5 which relates stiffness to the reduced modulus (i.e. the effective modulus which takes into account the elastic modulus of the sample and of the tip and contact area, A).

$$a = \left(\frac{3PR}{4E^*}\right)^{1/3} \tag{4}$$

$$K_s = \frac{2}{\sqrt{\pi}} E^* \sqrt{A}, \tag{5}$$

Where E^* is the reduced modulus as determined by

$$\frac{1}{E^*} = \frac{1 - \nu_s^2}{E_s} + \frac{1 - \nu_i^2}{E_i}. \tag{6}$$

The substitution of Equation 4 into Equation 5 and solving for E^* results in Equation 7 which, lastly, provides a means for converting the stiffness map—given that the four assumptions of Hertz's elastic contact theory hold—into an elastic modulus map using the applied scan load, P, the radius of the tip, R, and the stiffness of the contact, K_s.

$$E = \sqrt{\frac{K_s^3}{6PR}} \tag{7}$$

Once again, Equation 7 hinges on the four assumptions listed above. Since the first three assumptions all hinge on $a \ll R$, the validity of these three assumptions require close examination. For the applicability of the Hertz's models, the deformation between the tip and sample must consist of only elastic deformation. Combining Hertz's model for the maximum contact pressure, p_o, shown in Equation 8, and von Mises yield criterion, shown in Equation 9, for a material with $\upsilon = 0.3$ and yield strength Y, provides the maximum permissible force, Equation 10, for which the sample can be considered a purely elastic half-space.

$$p_o = \frac{3P}{2\pi a^2} = \left(\frac{6PE^{*2}}{\pi^3 R^2}\right) \tag{8}$$

$$(p_o)_y = 1.60\ Y \tag{9}$$

$$P_y = \frac{\pi^3 R^2}{6E^{*2}} (p_o)_y \tag{10}$$

Scanning Tip: R (nm)=500 E (GPa)= 1141 v = 0.07							
Material	**Elastic Modulus**	E^*	**Yield Strength**	**Poisson's Ratio**	$(\rho o)y$	**Onset of Plasticity** (P_Y)	**Upper limit for a fully plasticity contact**
	GPa	**GPa**	**MPa**		**MPa**	**µN**	**µN**
Copper (annealed)[1]	120.7	122.8	69	0.35	110.4	0.0001	0.05
Copper (spring temper)[1]	120.7	122.8	345	0.35	552	0.014	5.8
Carbon Steel 1010 (hot rolled)[1]	206.8	189.7	179	0.3	286.4	0.001	0.34
Carbon Steel 1010 (cold rolled)[1]	206.8	189.7	303	0.3	484.8	0.004	1.6
Stainless Steel 301 (hot rolled)[1]	189.6	174.4	276	0.28	441.6	0.004	1.5
Stainless Steel 301 (cold rolled)[1]	189.6	174.4	1138	0.28	1820.8	0.256	102.5
Polycarbonate[2]	2.3	2.7	65	0.37	104	0.206	82.2
PMMA[2]	3	3.6	80	0.4	128	0.214	85.5
Carbon Fiber	75	73.1	3000	0.2	4800	26.7	10683.0

1) Properties taken from R.L. Norton [4] 2) Properties provided by www.goodfellow.com [5]

Table 1: Elastic limit for some common engineering materials when tested using an indentation tip that has a nominal 500 nm tip radius.

The load values for the onset of plasticity for some common engineering materials using a tip that has a nominal spherical radius of 500 nm are provided in Table 1.

In many cases the forces that cause onset of plasticity, listed in Table 1, are lower than the resolutions of commercially available nanoindenters. All of the load limits for purely elastic contact, except for the carbon fiber sample, are impractical scan loads for nanoindenter systems. Only when the force is approximately 10X the load for the onset of plasticity do some of the materials come into the applicable load range for stiffness mapping. Increasing the tip radius can extend the elastic range for these materials, but not until the radius of the tip is increased to 100 µm are all of the materials listed in Table 1 within the acceptable load range (> 2 µN) for maintaining an elastic contact while scanning with a harmonic force imposed. The major disadvantage of using the larger tip radii is the loss of spatial resolution.

Table 1 also includes the approximate upper-limit for the load at which fully plastic deformation occurs assuming the materials are elastic-perfectly plastic materials. Johnson provides the approximation for the upper limit as

$$\frac{P}{P_y} \approx 400. \qquad (11)$$

Very little, if anything, is known about the applicability of Hertz's elastic contact equations between the first point of yield and fully plastic deformation. Stiffness maps on materials with low E/Y ratios show the most promise for conversion into mechanical properties maps. However, in addition to plasticity at higher loads, assumptions of single point contact and small strains become invalid. Surface roughness causes localized stress and plasticity. In polymers the contact radius grows rapidly violating the second assumption of small strains. As an example, the strain in the polymer samples at the onset of plasticity is already greater than 1% (using the approximation $\epsilon_R \approx \frac{0.2a}{R}$).

The discussion above is limited to the theory of elastic contact; however, many more challenging obstacles are encountered when working with non-ideal samples and tips. These challenges are listed below with only short explanations.

i) Maintaining a known contact force over the duration of a stiffness map: High resolution stiffness maps require between 1 and 2 hours of testing time and during this time the tip is kept in contact

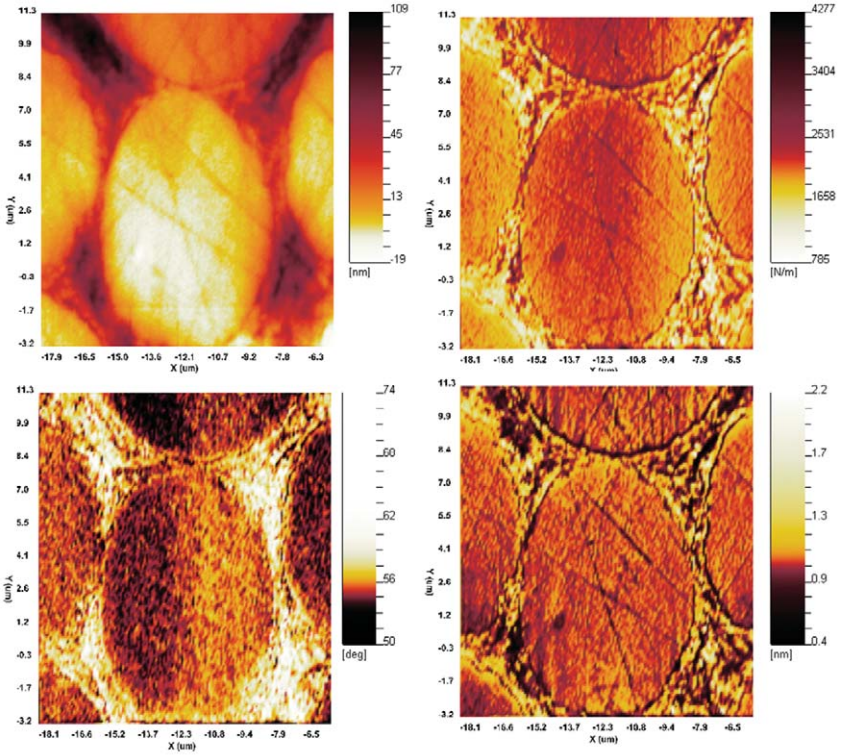

Figure 3. Dynamic imaging of a carbon fiber composite: topography (top left), stiffness (top right), phase angle (bottom left), and harmonic displacement (bottom right).

with the sample. Even with drift rates as low as 0.05 nm/s (this is an industry standard drift specification), the displacement change during a scan can easily be 360 nm. The assumption here is that any change in displacement is due to either a change in sample topography or drift while elastic contact is maintained with the sample. Table 1 shows that the assumption of a purely elastic contact is probably unfounded on most interesting samples and the challenge arises in decoupling the topography/drift/plasticity displacement changes—they all appear the same to the instrument. Therefore, the force will be adjusted incorrectly based on any plasticity in the contact and the error in contact force will grow with time.

ii) Surface roughness can cause large errors due to multiple points of contact between the sphere and the sample, producing unknown deformations which in no way resemble the single point of contact modeled by Hertz. Contact with surface roughness can easily induce plasticity into the contact which results in the load being inappropriately adjusted based on the assumption that only an elastic contact is being made. In application, the raw force of the instrument will be increased when plasticity occurs because the instrument senses that the displacement has dropped; therefore additional force is needed to maintain contact with the sample.

iii) Lastly, small spherical tips are difficult to manufacture - especially small diamond spherical tips for which the microstructure of diamond does not lend itself to a smooth spherical shape. Bushby et al. have shown that the radius of a diamond sphere is not constant with depth of penetration [4]. Therefore, when R is specified experimentally it is an effective R for which the contact, modeled as an elastic half space, can vary greatly.

To conduct quantitative mechanical properties maps, individual indentations should be performed and the properties should be measured using techniques that account for plasticity; the primary difference in these techniques are that they require measurements of penetration depth so that the amount of plasticity can be modeled. For these reasons the stiffness maps that are conducted in this article using contact scanning are not converted to mechanical properties maps using Hertz's equations and, instead, the collected data are evaluated for value as an alternative imaging technique.

Results and Discussion

The carbon fiber samples were scanned using a cube-corner tip with a nominal tip radius of 25nm. Using the same equations for the calculations performed in Table 1, the onset of plasticity for the carbon fibers using a tip with a 25 nm radius would occur at approximately 70nN and full plasticity would have an upper limit of 27μN. The sample was scanned using a scanning load of approximately 3 μN and a harmonic load oscillation between 1.5 and 2.5 μN. Therefore, undoubtedly some plasticity occurred; however, the results from the scan show that the contact was primarily dominated by elasticity. Figure 3 shows the topography, stiffness, phase angle, and harmonic displacement maps for the carbon fiber sample. The contact stiffness of

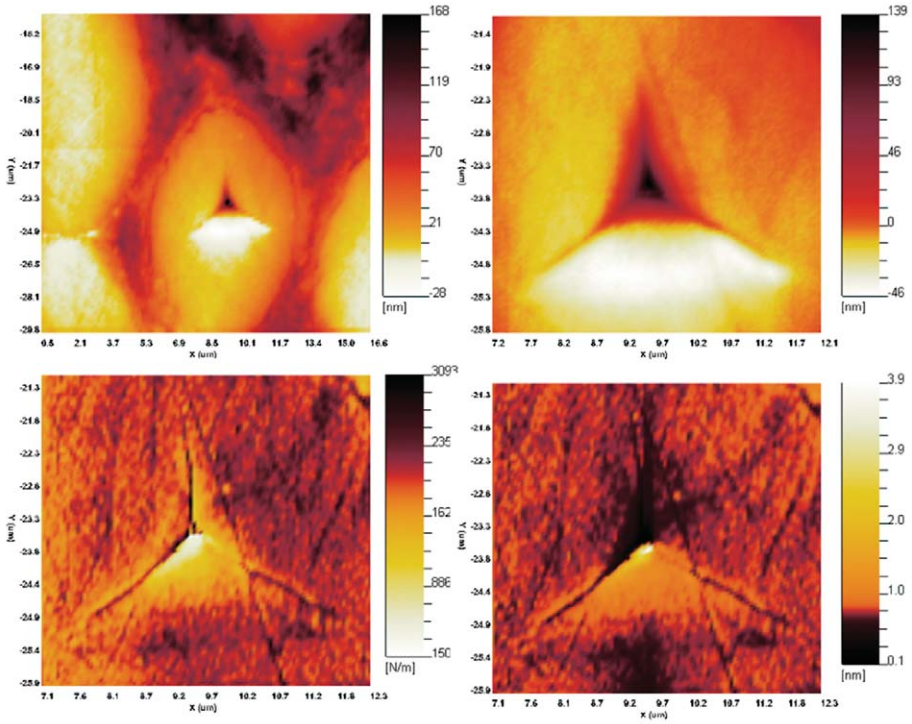

Figure 4. Dynamic image of a 1,500 nm indent in a carbon fiber: carbon fiber and indent topography (top left), indent topography (top right), stiffness map (bottom left), and harmonic displacement map (bottom right).

the carbon fibers ranged from 1995 N/m to 2810 N/m, while the epoxy region had a stiffness range from 1200 N/m to 4200 N/m. The stiffness range for the carbon fibers were in the expected range for materials with an elastic modulus between 65 and 100 GPa. However, the surrounding epoxy matrix shows stiffness values way out of the expected range because the stiffness measurement was dominated by surface roughness. When the topography map is examined next to the stiffness map as displayed in Figure 3, it is evident that stiffness is a convoluted measurement of contact area and mechanical properties, of which the contact area is strongly affected by surface roughness and plasticity. The dominate factor in the change of stiffness in the epoxy region of this sample was the surface roughness as opposed to the change in mechanical properties. Even the carbon fibers show this affect of surface roughness; scratches that were caused by the mechanical polishing process have a statistically different stiffness even though the scratch depths are at most 10 nm deep and approximately 600 nm wide. The graph of harmonic displacement details this even further because it is more sensitive to abrupt changes in contact area.

If the data collected in Figure 3 were assumed to conform to all of the assumptions listed in Hertz's elastic contact theory, then Equation 7 could be used to convert the scan into an elastic modulus map. Even though the contact appeared to be dominated by elasticity when scanning the carbon fibers, the scratches and topography change in the carbon fiber sample makes it difficult to assume a single point of contact. It is also apparent that there is a stiffness gradient on the right side of the center carbon fiber sample that corresponds directly to a topographical change– this is due to changes in tip contact as it is scanned across a surface that is not always orthogonal to the indenter. In conversion to a modulus map this stiffness gradient would be incorrectly construed as a gradient in elastic modulus. In addition, the assumption of single point contact and $a << R$ are clearly invalid in the epoxy region. Therefore, these data are not converted to mechanical properties maps in this article.

The sensitivity in stiffness measurements to abrupt increases in contact area caused by scratches or valleys gives rise to an excellent imaging technique for detecting minor fractures or impressions in indentation tests. When imaging edge impressions and fractures, the contact area changes abruptly in very close proximity to these features while experiencing subtle or no change in the areas just removed from the feature. Figure 4 shows the image of a 1,500 nm deep indentation on one of the carbon fibers with subsequent stiffness and harmonic displacement

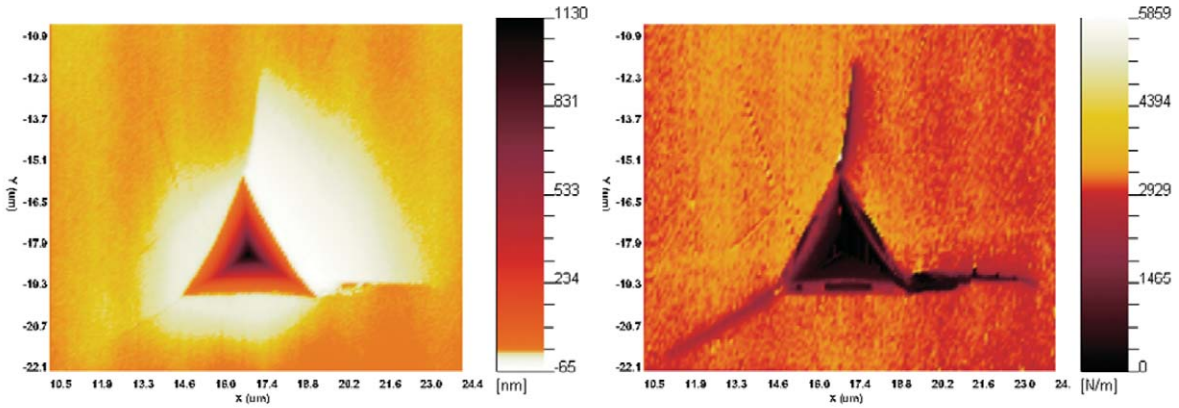

Figure 5. Topography (left) and stiffness map (right) of fracture in fused silica. The stiffness map clearly shows the length of crack propagation.

maps of the region surrounding the indentation. This indentation was produced using a cube corner-tip to create higher amounts of plasticity in the indent. The dynamic images of the indentation clearly show the edge impressions of the tip in the carbon fiber.

Measuring fracture during indentation with a cube-corner tip exemplifies the value of the dynamic imaging technique in detecting the length of crack propagation as would be done in fracture toughness measurements. Indentation tests were performed on fused silica to a load of 120 mN and a maximum penetration depth of 2,200 nm was reached. Figure 5 shows the dynamic scan results of topography and stiffness for one of the tests. Cracking during indentation on brittle materials is common when using a cube-corner tip because it displaces a large volume of material with respect to its contact area [7]. While the topographical image shows the cracking, it is difficult to determine the propagation length due to the diminishing crack width. Sensitivity in the stiffness measurements to small changes in contact area fixes this problem. The stiffness map in Figure 5 provides a contrast that allows easy measurement of the crack lengths and it is seen in the stiffness map that the cracks propagate further than can be determined from the topographical image. The two cracks in the lower corners of the indent are the most deceiving in the topography map because they appear to have clear end points until the map of stiffness reveals a small curve at the end of the bottom right crack and seemingly an unending crack for the bottom left. Stiffness mapping simply removes the guessing game from measuring crack lengths at the edge of indentations.

Conclusions

Due to the loads associated with the onset of plasticity in most materials and the required assumption of a single point contact, it is difficult to define a range of materials where it is acceptable to convert a stiffness map into a mechanical properties map when acquired through contact scanning. It was shown that even if the contact is dominated by elasticity, small changes in topography can cause large changes in the measured stiffness. Larger spheres could be used to extend the elastic range; however, with larger spheres comes lower resolution and the problems encountered due to surface roughness still exist. Stiffness mapping can be used effectively to examine small scale fracture and impressions where topographical images lack stark contrast. When the tip scans across a region of abrupt topography change, the stiffness change is dramatic. This type of image contrast allowed the examination of small scale fractures in fused silica that would typically required atomic force or scanning electron microscopy to appropriately measure the crack length.

References

[1] http://www.engr.utk.edu/mse/Textiles/CARBON%20FIBERS.htm

[2] Pharr, G.M., Strader, J.H., Oliver, W.C. "Critical issues in making small-depth mechanical property measurements by nanoindentation with continuous stiffness measurement." *Journal of Materials Research* 24 (2009): 653–666.

[3] K.L. Johnson. *Contact Mechanics.* New York: Cambridge University Press, 1985.

[4] R.L. Norton. *Machine Design An Integrated Approach, 2nd Edition.* Upper Saddle River: Prentice-Hall, 1998.

[5] www.goodfellow.com

[6] Bushby, A.J. and Jennett, N.M. *MRS Symposium Proceeding.* **649**, (2001), Q7.17.1–6.

[7] Pharr, G.M., Harding, D.S., and Oliver, W.C. "Measurement of fracture toughness in thin films and small volumes using nanoindentation methods." In: M. Nastasi, D.M. Parkin and H. Gleiter Editors, *Mechanical Properties and Deformation Behavior of Materials having Ultra-fine Microstructures NATO ASI Series E: Applied Sciences* **233** Kluwer, Dordrecht (1993), pp. 449–461

Nano Mechanical Systems from Agilent Technologies

Agilent Technologies, the premier measurement company, offers high-precision, modular nano-measurement solutions for research, industry, and education. Exceptional worldwide support is provided by experienced application scientists and technical service personnel. Agilent's leading-edge R&D laboratories ensure the continued, timely introduction and optimization of innovative, easy-to-use nanomechanical system technologies.

www.agilent.com/find/nanoindenter

Americas

Canada	(877) 894 4414
Latin America	305 269 7500
United States	(800) 829 4444

Asia Pacific

Australia	1 800 629 485
China	800 810 0189
Hong Kong	800 938 693
India	1 800 112 929
Japan	0120 (421) 345
Korea	080 769 0800
Malaysia	1 800 888 848
Singapore	1 800 375 8100
Taiwan	0800 047 866
Thailand	1 800 226 008

Europe & Middle East

Austria	43 (0) 1 360 277 1571
Belgium	32 (0) 2 404 93 40
Denmark	45 70 13 15 15
Finland	358 (0) 10 855 2100
France	0825 010 700*
	*0.125 €/minute
Germany	49 (0) 7031 464 6333
Ireland	1890 924 204
Israel	972-3-9288-504/544
Italy	39 02 92 60 8484
Netherlands	31 (0) 20 547 2111
Spain	34 (91) 631 3300
Sweden	0200-88 22 55
Switzerland	0800 80 53 53
United Kingdom	44 (0) 118 9276201

Other European Countries:
www.agilent.com/find/contactus

Printed in USA, October 6, 2011
5990-6329EN

Agilent Technologies